

# All-electron self-consistent GW approximation: Application to Si, MnO, and NiO

Sergey V. Faleev,<sup>1</sup> Mark van Schilfgaarde,<sup>2</sup> and Takao Kotani<sup>3</sup>

<sup>1</sup>Sandia National Laboratories, Livermore, CA 94551

<sup>2</sup>Arizona State University, Tempe, AZ, 85284

<sup>3</sup>Department of Physics, Osaka University, Toyonaka 560, Japan

(Dated: October 5, 2018)

We present a new kind self-consistent *GW* approximation (sc*GW*) based on the all-electron, full-potential LMTO method. By iterating the eigenfunctions of the *GW* Hamiltonian, self-consistency in both the charge density and the quasiparticle spectrum is achieved. We explain why this form of self-consistency should be preferred to the conventional one. Then some results for Si are shown as a representative semiconductor, to establish agreement with a prior sc*GW* calculation. Finally we consider many details in the electronic structure of the antiferromagnetic insulators MnO and NiO. Excellent agreement with experiment is shown for many properties, suggesting that a Landau quasiparticle (energy band) picture of MnO and NiO provides a reasonable description of electronic structure even in these correlated materials.

PACS numbers: 71.15.-m,71.15.Ap,71.20.-b,75.50.Ee

The *GW* approximation (GWA) of Hedin[1] is generally believed to accurately predict excited-state properties, and in particular improve on the local density approximation (LDA), whose limitations are well known, e.g. to underestimate bandgaps semiconductors and insulators. Usually GWA is computed as 1-shot calculation starting from the LDA eigenfunctions and eigenvalues; the self-energy  $\Sigma$  is approximated as  $\Sigma = iG^{\text{LDA}}W^{\text{LDA}}$ , where  $G^{\text{LDA}}$  is a bare Green function constructed from LDA eigenfunctions, and  $W^{\text{LDA}}$  is the screened Coulomb interaction constructed from  $G^{\text{LDA}}$  in the random phase approximation (RPA). However, establishing the validity of the 1-shot approach has been seriously hampered by the fact that nearly all calculations to date make further approximations, e.g. computing  $\Sigma$  from valence electrons only; the plasmon-pole approximations; and the pseudopotential (PP) approximation to deal with the core. Only recently when reliable all-electron implementations have begun to appear, has it been shown that the 1-shot GWA with PP leads to systematic errors[2, 3, 4]. There is general agreement among the all-electron calculations (see Table I) that the  $\Gamma$ -X transition in Si is underestimated when  $\Sigma = iG^{\text{LDA}}W^{\text{LDA}}$ . And we have shown previously[2] that the tendency for  $\Sigma = iG^{\text{LDA}}W^{\text{LDA}}$  to underestimate gaps is almost universal in semiconductors. This is reasonable because  $W^{\text{LDA}}$  overestimates the screening owing to the LDA small band gaps.  $G$  constructed from quasiparticles (QP) with a wider gap (e.g. a self-consistent  $G$ ) reduces the screening, and therefore generates *GW* with a wider gap.

However, there are many possible ways to achieve self-consistency. The theoretically simplest (and internally consistent) is the fully self-consistent scheme (sc*GW*), which is derived through the Luttinger-Ward functional with the exchange-correlation energy approximated as the sum of RPA ring diagrams. Then  $W$  is evaluated as  $W = v(1 - vP)^{-1}$  with the proper part of the polar-

ization function  $P = -iG \times G$ . However, such a construction may not give reasonable  $W$  [5], resulting in a poor  $G$ , for the following reason. If  $\Sigma$  is  $\omega$ -dependent,  $G$  can be partitioned into a QP part and a residual satellite part. The QP part consists of terms whose energy-dependence varies as  $Z_i/(\omega - \epsilon_i \pm i\Gamma_i)$ , where  $\epsilon_i$ ,  $\Gamma_i$ , and  $Z_i$  are respectively the QP energies, inverse lifetimes, and renormalization factors ( $Z_i < 1$ ; typically between 0.7 and 1). The QP parts are thus weighted by factors  $Z$ ; the residual weights  $1 - Z$  go into the plasmon-related satellite parts, high in energy. Thus  $P = -iG \times G$  contains contributions from the particle-hole pair excitations as does  $-iG^{\text{LDA}} \times G^{\text{LDA}}$ , but reduced by the products of two  $Z$  factors, one from occupied and the other from unoccupied states. However, this construction of  $P$  is not consistent with Landau's quasi-particle theory, which insists that one-particle excitations remain meaningful (at least near the Fermi energy). Based on the theory, we should instead evaluate the QP contributions to  $P$  without  $Z$  factors, as they dominate the static screening  $W(\omega \rightarrow 0)$ . Inclusion of  $Z$  can lead to  $W(0)$  being underscreened; moreover  $W(\omega)$  does not satisfy the  $f$  sum rule [5]. Consequently  $W(0)$  will be overestimated resulting in a tendency to overestimate band widths, as is well known in the extreme case (Hartree-Fock), where there is no screening of  $W$ .

Indeed Holm found that sc*GW* overestimates the band width in the homogeneous electron gas[6]. Very recently Ku presented a sc*GW* calculation which similarly overestimates the valence band width in Si and Ge; see Table I [4]. Another practical justification for the argument that a bare  $G$  without  $Z$  should be used when we construct  $P$  as  $-iG \times G$ , is that  $W^{\text{LDA}}$  is already known to be rather good if we add some enlargement of band gap by hand to correct for errors in the LDA  $\epsilon_i$  [7].

For this reason, we do not adopt the full sc*GW* scheme, but construct two kinds of constrained self-consistent *GW* methods. For a set of trial eigenfunctions and

quasi-particle energies  $\{\psi_{\mathbf{q}n}, \epsilon_{\mathbf{q}n}\}$ , we can calculate the one-particle Green function  $G$ , from which we can calculate self-energy  $\Sigma_{nn'}^{\mathbf{q}}(\omega)$  in the expansion of  $\{\psi_{\mathbf{q}n}\}$  in the GWA. Then we generate an energy-independent and hermitian  $\Sigma_{nn'}^{\mathbf{q}}$  in one of two ways:

$$\Sigma_{nn'}^{\mathbf{q}} = \Sigma_{nn'}^{\mathbf{q}}(E_F) + \delta_{nn'} \text{Re}[\Sigma_{nn}^{\mathbf{q}}(\epsilon_{\mathbf{q}n}) - \Sigma_{nn}^{\mathbf{q}}(E_F)] \quad (1)$$

$$\Sigma_{nn'}^{\mathbf{q}} = \text{Re} \left[ \Sigma_{nn'}^{\mathbf{q}}(\epsilon_{\mathbf{q}n}) + \Sigma_{nn'}^{\mathbf{q}}(\epsilon_{\mathbf{q}n'}) \right] / 2 \quad (2)$$

where  $\text{Re}$  means that we take only the hermitian parts. With this  $\Sigma_{nn'}^{\mathbf{q}}$ , we can construct a new density  $n(\mathbf{r})$  and corresponding Hartree potential, and proceed to a new set of  $\{\psi_{\mathbf{q}n}, \epsilon_{\mathbf{q}n}\}$ . The procedure can be iterated to self-consistency. Our method is not related to the LDA (though in practice the LDA is used to make a starting guess for  $\Sigma$  and the augmented-wave basis set). These two schemes differ in the treatment of the off-diagonal parts of  $\Sigma_{nn'}$ ; but both restrict the potential to be non-local, hermitian and  $\omega$ -independent. Thus the problem in the full *scGW* is avoided; also the numerical computation becomes rather stable. In Ref.[4], off-diagonal matrix elements of  $\Sigma_{nn'}^{\mathbf{q}}$  were completely neglected. However, these are important for MnO and NiO: eigenfunctions and the density can not be changed from LDA if we neglect them. We find that converged QP energies differ in these two schemes by small amounts (less than  $< 0.02$  eV for Si, typically  $\sim 0.1$  eV for NiO), which is within the resolution of the method ( $\sim 0.1$  eV).

Our implementation is based on the method of Ref. [2].  $W$  is expanded in a mixed basis which consists of two contributions, local atom-centered functions (product basis) confined to muffin-tin spheres, and plane waves with the overlap to the local functions projected out. The former can include any of the core states: thus the valence and core states can be treated on an equal footing and the contribution of the latter to  $\Sigma$  included. We calculate the full energy dependence of  $W$  without the plasmon-pole approximation. This approach shares some features in common with both the full-potential, all-electron plane-wave based methods[3, 4] and the product-basis method[8], combining the advantages of each, e.g. efficient treatment of localized valence electrons.

Results for Si are shown in Table I. Agreement between the three all-electron methods is generally excellent. The  $G^{\text{LDA}}W^{\text{LDA}}$  gaps are  $\sim 0.3$  eV smaller than experiment; the *scGW* gaps fall much closer. As we will show elsewhere, most properties of weakly correlated systems calculated with the present *scGW* method (fundamental and higher-lying gaps, valence bandwidths, effective mass, position of deep  $d$  levels) are in excellent agreement with experiment, with small but systematic residual errors.

Turning to the TM oxides, we first consider MnO because it is less correlated. Fig. 1 compares the *scGW* energy bands and corresponding DOS to the LDA and the  $G^{\text{LDA}}W^{\text{LDA}}$  gap. The conduction band at  $\Gamma$  is evidently

TABLE I: Minimum energy gap  $E_g$  and selected energy eigenvalues for Si, relative to  $\Gamma_{25v}$  (eV). Three all-electron methods are shown: linearized augmented-plane-wave (LAPW) and projector-augmented-wave (PAW) approaches, and LMTO (this work). The PAW calculation included valence electrons only. The last row compares the Ge valence bandwidth. The results of this work differ slightly from Ref. [2] because a large basis set (50 orbitals/atom) was employed in the present work.

	PAW[3] ( $GW$ ) <sup>LDA</sup>	LAPW[4] ( $GW$ ) <sup>LDA</sup>	scGW	This work ( $GW$ ) <sup>LDA</sup>	scGW	Exp.
$E_g$	0.92	0.85	1.03	0.92	1.14	1.17
$X_{1c}$	1.01			1.06	1.30	1.32
$L_{1c}$	2.05			2.00	2.26	2.04
$\Gamma_{15c}$	3.09	3.12	3.48	3.11	3.40	3.38
$\Gamma_{1v}$		-12.1	-13.5	-12.1	-12.3	-12.5
$\Gamma_{1v}(\text{Ge})$		-13.1	-14.8	-12.9	-13.1	-12.6

a dispersive band of  $sp$  character. Above this, fall the  $t_{2g}$  bands ( $\sim 6$ -9 eV); still higher at  $\sim 10$  eV is a narrow  $e_g$  band, whose width is  $\sim 3$  eV. Thus, the itinerant and  $d$  bands are well separated. The minimum gap is 3.5 eV, in good agreement with the BIS gap[9] ( $3.9 \pm 0.4$  eV). The BIS spectrum also shows a peak at  $\sim 6.8$  eV, which probably corresponds to a convolution of the peaks of  $t_{2g}$  symmetry seen in the DOS at 6.6 eV and 7.3 eV. These bands are in stark contrast to the LDA, which shows the  $t_{2g}$  and  $e_g$  bands overlapping and hybridizing with the  $sp$  band at 1 to 4 eV.

LDA and *scGW* valence bands are more similar (Fig. 1). In the LDA there is a narrow upper  $e_g$  band at 0.1 eV below the valence band maximum (VBM), and another one at  $\text{VBM}-5$  eV. Both weakly hybridize with the O  $2p$  band. The *scGW* pushes the upper  $e_g$  band down to  $\text{VBM}-0.5$  eV, so that the VBM takes more O  $2p$  character, and the band at  $\text{VBM}-5$  eV takes more Mn  $d$  character. The splitting  $\Delta_v$  between the upper  $e_g$  level and the  $t_{2g}$  level widens from 1.0 eV(LDA) to 1.7 eV(*scGW*), in good agreement a photoemission measurement of 1.9 eV[9]. An approximately similar picture emerges from a model *GW* calculation of Massidda[10], the most important difference being that the model *GW*  $d$  conduction bands fall  $\sim 1$  eV lower than ours.

Fig. 2 compares the *scGW* energy bands for NiO along the  $[110]$  and  $[100]$  lines to ARPES data of Shen [11] for the valence bands, and to the LDA conduction bands. The right panel shows the density-of-states (DOS) for both LDA and *scGW*, and Fig. 3 shows the total DOS resolved into components. Also shown in the top panel are BIS data taken from Ref. 12.

Several features are of interest:

1. The conduction-band minimum falls at the  $\Gamma$  point; the VBM falls at the point  $(1/2, 1/2, 1/2)$  (not shown). The calculated minimum gap is 4.8 eV.
2. The *scGW* conduction bands are a mixture of a disper-

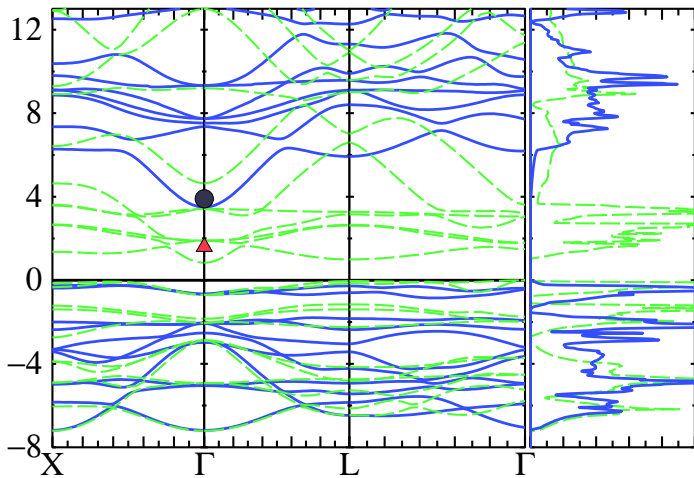


FIG. 1: scGW energy bands and DOS of MnO. Solid lines: scGW bands; dashed lines: LDA bands. The VBM is set to energy 0. Circle and triangle at  $\Gamma$ : BIS and  $G^{\text{LDA}}W^{\text{LDA}}$  gaps. Right panel shows the corresponding DOS. Peaks at -0.5 eV (-0.1 eV in LDA) and -5 eV are the nearly dispersionless  $e_g$  bands. Peaks at -2.2 eV (-1.2 eV) and 6.6 and 7.3 eV (1.7 and 1.9 eV) derive from Mn  $t_{2g}$  states.

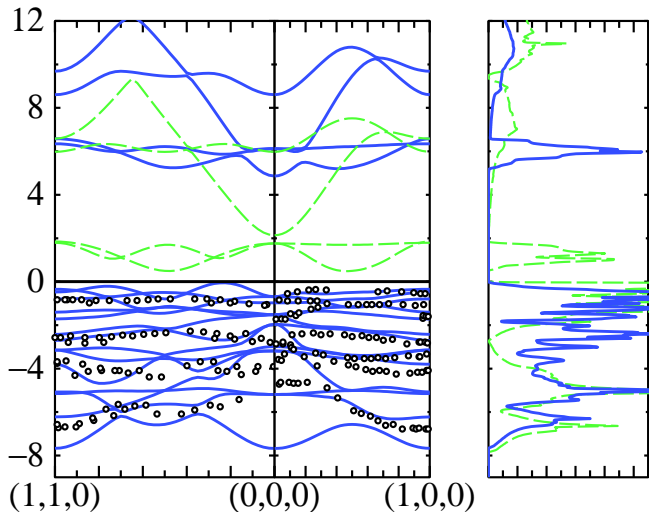


FIG. 2: scGW energy bands and DOS of NiO. Valence-band maximum is set at energy 0. Solid lines: scGW bands; dashed lines: LDA bands (only conduction bands are shown). Circles show photoemission data of Ref. 11. Right panel shows the corresponding total DOS.

sive band composed of  $sp$  approximately equally weighted on the Ni and O sites, and a nearly dispersionless  $e_g$  state (see discussion of EELS, below). Peaks in the BIS spectrum labeled ‘1’, ‘2’ and ‘3’ closely coincide to those in the scGW total DOS, apart from a constant shift of 0.8eV.

3. The scGW valence bands are in very good agreement with experiment: indeed they agree as well with the Shen data as the latter agrees with an independent experiment by Kühlenbeck et. al.[14] (not shown).

4. There is an increased dispersion in the valence bands

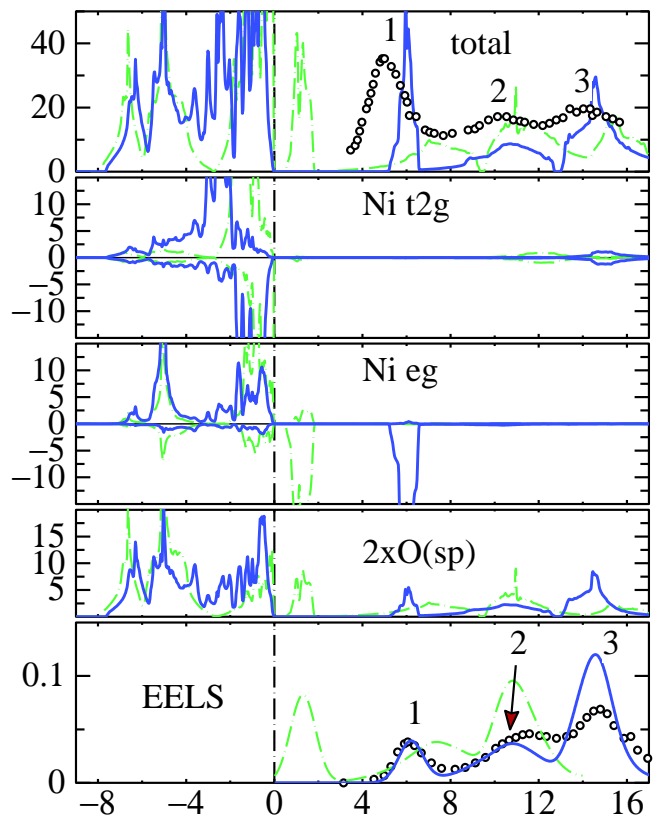


FIG. 3: DOS and EELS of NiO. Solid lines: scGW data; dashed lines: LDA data. Top panel: total DOS, together with BIS data of Ref. 12 (circles). Panels 2 and 3 show the Ni  $t_{2g}$  and  $e_g$  partial DOS, with positive DOS showing majority spin and negative showing minority spin. Panel 4 shows the O  $sp$  partial DOS; panel 5 compares the calculated and measured[13] EELS spectra from the O 1s level.

relative to the LDA at the VBM because the nearly dispersionless Ni  $t_{2g}$  levels are pushed down. Thus the VBM acquires somewhat more O 2p character. This supports the generally accepted picture that the LDA too heavily favors the Mott-Hubbard picture.

The bottom panel of Fig. 3 compares the EELS spectrum calculated as described in Ref. 15, computing the excitation from the O 1s core. Calculated data were convolved by a Gaussian of 0.5 eV width (which was the resolution reported) to compare to experimental data by reported by Dudarev et. al.[13]. The calculated results were shifted to align the spectra with the DOS. For purposes of comparison, Dudarev’s data was shifted by 526 eV to align the peaks with the scGW results. (Peaks labeled ‘1’, ‘2’ and ‘3’ should correspond to the peaks with the same labels in the BIS spectrum; indeed the EELS peaks and BIS peaks almost perfectly align if the EELS data is further shifted by 0.8 eV.)

Apart from the 0.8 eV shift, the EELS data is in excellent agreement with the scGW results. Spacings between the three peaks agree to within  $\sim 0.1$  eV, and the

spectral weight under each peak (estimated by numerical integration) also agree closely. This establishes that the *scGW* relative positions of the *sp* and Ni *d* bands are correctly predicted. This is a significant result, because the relative positions of the *sp* and *d* bands is a rather a delicate quantity[16]. In contrast, the LDA underestimates the spacings between peaks 1 and 2 by  $\sim 1.5$  eV and between peaks 2 and 3, by  $\sim 0.7$ . Moreover, it overestimates the spectral weight of the first peak by a factor of  $\sim 2$ . This result is also significant, because the EELS spectra largely reflect the O *2p* partial DOS. Without coupling between the Ni  $e_g$  level, the itinerant band would adopt a simple parabolic form; thus the amplitude of first peak is a reflection of the hybridization between the Ni  $e_g$  and the itinerant band. The fact that *scGW* gets the correct weight for this peak establishes that it accurately estimates this coupling, while the LDA overestimates it by a factor of 2.

Many of the results found here confirm many conclusions drawn in a model *GW* calculation [17], as well as various LDA+*U* calculations[13, 18, 19], both of which may be viewed as model approaches to the present theory. Some significant differences do arise. The relative positions of different bands and the energy gaps depend rather sensitively on the choice of parameters in the model approaches. For example, in Ref. [19], the O-derived *sp* conduction-band appears to fall at 2.8 eV,  $\sim 2$  eV below the middle of the  $e_g$  level when *U* is assumed to be 5 (somewhat lower than the constrained LDA estimate,  $U \sim 8$  eV). Massidda's model *GW* calculation[17] shows the *sp* band  $\sim 1$  eV above the  $e_g$ .

To what extent does the Landau QP picture based on the preceding *scGW* results fail to describe the true electronic structure of MnO and NiO? We have shown that a great deal is correctly described, including many details of the valence and conduction bands. The main discrepancy is with XPS measurements. For optics, the peak in  $\text{Im}(\epsilon)$  corresponding to the gap in NiO is about VBM+4 eV whereas this peak is at VBM+5 eV in the BIS data. But  $\text{Im}(\epsilon)$  is directly related to the excitonic process or correlational motion of electron-hole pair. Such a correlation can shift  $\text{Im}(\epsilon)$  downward. The difference between the two experiments can be due to this correlation. So the poles of the true Green's function (which are reflected in the DOS) should correspond to the unoccupied *d* position at VBM+5 eV as is shown in BIS. Peak '1' in the *scGW* DOS falls slightly higher than experiment, at  $\sim 5.8$  eV. If we include correlation beyond RPA, e.g. inclusion of ladder diagrams, the band gap in the Green's function may be reduced about 1 eV, as estimated by Takahashi and Igarashi[20]. Thus, it would seem that the RPA explains quite well the important experimental data, apart from a slight tendency to underestimate screening of *W*[21]. We have not yet attempted to include excitonic effects, so we cannot say to what extent photoemission data can be explained within

TABLE II: Magnetic moments and minimum gaps in MnO and NiO.

Compound	moment			bandgap		
	LDA	<i>scGW</i>	Expt	LDA	<i>scGW</i>	Expt
MnO	4.48	4.76	4.6	0.78	3.5	$3.9 \pm 0.4$
NiO	1.28	1.72	1.9	0.45	4.8	4.3

the RPA, though estimates in a model context were reasonably successful[18]. Thus, we believe that the band picture[22] for NiO is a reasonable starting point for the description of the electronic structure of NiO, much better than previously thought, and in many respects more appropriate than the ligand-field picture.

This work was supported by the Office of Naval Research.

- 
- [1] L. Hedin, Phys. Rev. **140**, A796 (1965).
  - [2] T. Kotani and M. van Schilfhaarde, Sol. State Commun. **121**, 461 (2002).
  - [3] S. Lebegue, B. Arnaud, M. Alouani, and P. Bloechl, Phys. Rev. B **67**, 155208 (2003).
  - [4] W. Ku and A. G. Eguiluz, Phys. Rev. Lett. **89**, 126401 (2002).
  - [5] D. Tamme, R. Schepe, and K. Henneberger, Phys. Rev. Lett. **83**, 241 (1999).
  - [6] B. Holm and U. von Barth, Phys. Rev. B **57**, 2108 (1998).
  - [7] B. Arnaud and M. Alouani, Phys. Rev. B **63**, 085208 (2001).
  - [8] F. Aryasetiawan and O. Gunnarsson, Rep. Prog. Phys. **61**, 237 (1998).
  - [9] J. van Elp, R. H. Potze, H. Eskes, R. Berger, and G. A. Sawatzky, Phys. Rev. B **44**, 1530 (1991).
  - [10] S. Massidda, A. Continenza, M. Posternak, and A. Baldereschi, Phys. Rev. Lett. **74**, 2323 (1995).
  - [11] Z.-X. Shen, R. S. List, D. S. Dessau, B. O. Wells, O. Jepsen, A. J. Arko, R. Bartlett, C. K. Shih, F. Parmigiani, J. C. Huang, et al., Phys. Rev. B **44**, 3604 (1991).
  - [12] G. A. Sawatzky and J. W. Allen, Phys. Rev. Lett. **53**, 2339 (1984).
  - [13] S. L. Dudarev, G. A. Botton, S. Y. Savrasov, C. J. Humphreys, and A. P. Sutton, Phys. Rev. B **57**, 1505 (1998).
  - [14] H. Kuhlbeck, G. Odorfer, R. Jaeger, G. Illing, M. Menges, T. Mull, H.-J. Freund, M. Pohlchen, V. Staemmler, S. Witzel, et al., Phys. Rev. B **43**, 1969 (1991).
  - [15] A. T. Paxton, M. van Schilfhaarde, M. MacKenzie, and A. J. Craven, J. Phys. C p. 729 (2000).
  - [16] To achieve this result, it was essential to use a well-converged basis set, in particular including local orbitals on the Ni *d* sites. Without the local orbital the  $e_g$  falls at  $\sim 1-2$  eV higher energy.
  - [17] S. Massidda, A. Continenza, M. Posternak, and A. Baldereschi, Phys. Rev. B **55**, 13494 (1997).
  - [18] V. I. Anisimov, I. V. Solovyev, M. A. Korotin, M. T. Czyzyk, and G. A. Sawatzky, Phys. Rev. B **48**, 16929 (1993).

- [19] O. Bengone, M. Alouani, P. Blochl, and J. Hugel, Phys. Rev. B **62**, 16392 (2000).
- [20] M. Takahashi and J. Igarashi, Phys. Rev. B **54**, 13566 (1996).
- [21] Interestingly, the semiconductors also demonstrate a slight but universal tendency to overestimate the bandgaps; see, e.g. Ku's results for Ge[4]. Not surprisingly, the pair-correlation effect between electron-hole is rather larger in a correlated material such as NiO.
- [22] K. Terakura, T. Oguchi, A. R. Williams, and J. Kübler, Phys. Rev. B **30**, 4734 (1984).